Journal of African Earth Sciences 102 (2015) 233–246

Contents lists available at ScienceDirect

Journal of African Earth Sciences

journal homepage: www.elsevier.com/locate/jafrearsci

Active fault mapping in Karonga-Malawi after the December 19, 2009 Ms 6.2 seismic event

A.S. Macheyeki [a,*], H. Mdala [b], L.S. Chapola [c], V.J. Manhiça [d], J. Chisambi [b], P. Feitio [e], A. Ayele [f], J. Barongo [g], R.W. Ferdinand [h], G. Ogubazghi [i], B. Goitom [j], J.D. Hlatywayo [k], G.K. Kianji [g], I. Marobhe [h], A. Mulowezi [e,l], D. Mutamina [m], J.M. Mwano [a], B. Shumba [n], I. Tumwikirize [e,l]

[a] Geological Survey of Tanzania, P.O. Box 903, Dodoma, Tanzania
[b] Geological Survey of Malawi, P.O. 27, Zomba, Malawi
[c] The Catholic University of Malawi, Montfort Campus, P.O. Box 5452, Limbe, Malawi
[d] National Directorate of Geology, Mozambique
[e] Direccao Nacional de Geologia, Praca 25 de Junho, C.P. 217, Maputo, Mozambique
[f] Faculty of Sciences Geophysical Observatory, University of Addis Ababa, P.O. Box 1176, Ethiopia
[g] Department of Geology, University of Nairobi, Kenya
[h] Department of Geology, University of Dar Es Salaam, P.O. Box 35052, Dar Es Salaam, Tanzania
[i] Department of Earth Sciences, Eritrea Institute of Technology, Asmara, Eritrea
[j] School of Earth Sciences, University of Bristol, UK
[k] Applied Physics Department, National University of Science and Technology, Box AC939, Ascot, Bulawayo, Zimbabwe
[l] Ministry of Energy and Minerals Development, Geological Survey and Mines Department, P.O. Box 9, Entebbe, Uganda
[m] Geological Survey Department, P.O. Box 50135, Lusaka, Zambia
[n] The International Seismological Centre, Thatcham, UK

ARTICLE INFO

Article history:
Received 25 July 2014
Received in revised form 8 October 2014
Accepted 20 October 2014
Available online 1 November 2014

Keywords:
December 2009 seismic event
Active fault mapping
Fault segment
Karonga
Malawi

ABSTRACT

The East African Rift System (EARS) has natural hazards – earthquakes, volcanic eruptions, and landslides along the faulted margins, and in response to ground shaking. Strong damaging earthquakes have been occurring in the region along the EARS throughout historical time, example being the 7.4 (Ms) of December 1910. The most recent damaging earthquake is the Karonga earthquake in Malawi, which occurred on 19th December, 2009 with a magnitude of 6.2 (Ms). The earthquake claimed four lives and destroyed over 5000 houses. In its effort to improve seismic hazard assessment in the region, Eastern and Southern Africa Seismological Working Group (ESARSWG) under the sponsorship of the International Program on Physical Sciences (IPPS) carried out a study on active fault mapping in the region.

The fieldwork employed geological and geophysical techniques. The geophysical techniques employed are ground magnetic, seismic refraction and resistivity surveys but are reported elsewhere. This article gives findings from geological techniques. The geological techniques aimed primarily at mapping of active faults in the area in order to delineate presence or absence of fault segments. Results show that the Karonga fault (the Karonga fault here referred to as the fault that ruptured to the surface following the 6th–19th December 2009 earthquake events in the Karonga area) is about 9 km long and dominated by dip slip faulting with dextral and insignificant sinistral components and it is made up of 3–4 segments of length 2–3 km. The segments are characterized by both left and right steps.

Although field mapping show only 9 km of surface rupture, maximum vertical offset of about 43 cm imply that the surface rupture was in little excess of 14 km that corresponds with Mw = 6.4. We recommend the use or integration of multidisciplinary techniques in order to better understand the fault history, mechanism and other behavior of the fault/s for better urban planning in the area.

© 2014 Elsevier Ltd. All rights reserved.

1. Introduction

The East African Rift System (EARS) has natural hazards – earthquakes, volcanic eruptions, and landslides along the faulted margins, and in response to ground shaking. The most recent damaging earthquake in the Eastern and Southern Africa regions is the Karonga earthquake in Malawi, which occurred on 19th December, 2009 with a magnitude of Ms 6.2 (~Mw = 6.2). It was part of the 6th–19th December 2009 earthquake sequence in the area. The earthquake claimed 4 lives and destroyed over 5000

* Corresponding author.
E-mail address: asmacheyeki@yahoo.com (A.S. Macheyeki).

http://dx.doi.org/10.1016/j.jafrearsci.2014.10.010
1464-343X/© 2014 Elsevier Ltd. All rights reserved.

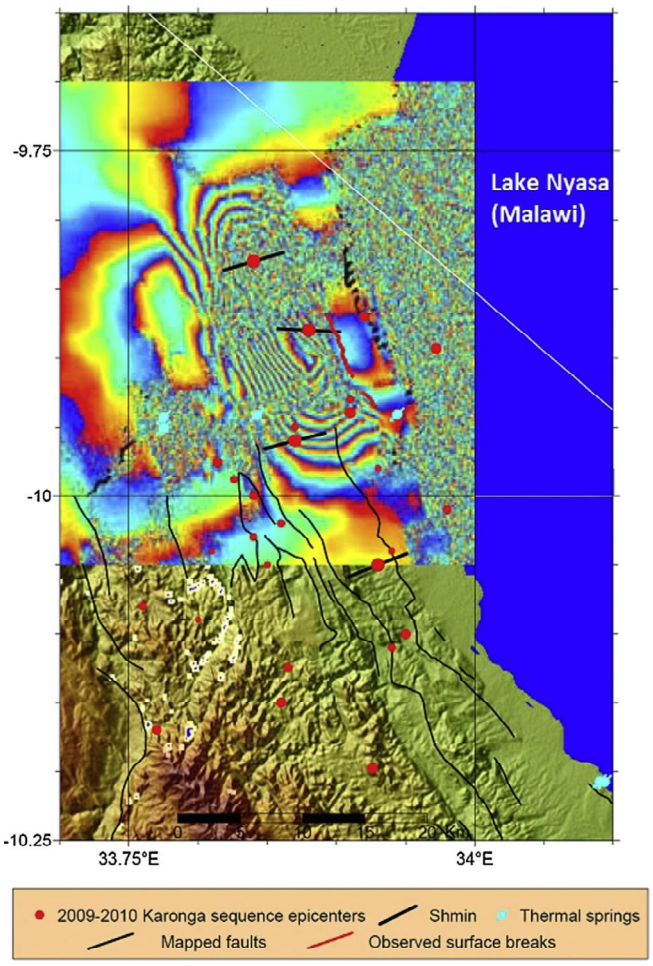


Fig. 1. Observed surface breaks (Karonga fault) versus the Envisat Interferograms (from Biggs et al., 2010) of the 2009 Karonga earthquake. An insert is the Tectonic map of East Africa (https://lh4.googleusercontent.com/-SnBOlRzHNK8/TXj5JrU565I/AAAAAAAABJI/kIpqSufYlkU/s1600/ear.gif).

houses (Malawi Geological Survey, 2009). The 2009 crisis reactivated secondary west-dipping faults, synthetic to the main Livingstone border fault (see Biggs et al., 2010; Hamiel et al., 2012; Fig. 1). The surface breaks occurred on the Quaternary plain relatively close to Lake Nyasa/Malawi, in an area that bears apparently no traces of previous rupture(s). For that reason, new seismic hazard assessment is required for the region.

Active fault data is one of the input parameters required in seismic hazard assessment because earthquake magnitudes are proportional to size of active faults (e.g. Wells and Coppersmith, 1994). Such kind of data is currently not available in the region. In its effort to improve seismic hazard assessment in the region, Eastern and Southern Africa Seismological Working Group (ESARSWG) under the sponsorship of the International Program on Physical Sciences (IPPS) carried out a project on active fault mapping in the Karonga-Malawi area. The project started in August 2009 with a desk study and was followed by reconnaissance survey in November 2009. Active fault mapping campaign was conducted in October 2010.

The fieldwork employed multidisciplinary techniques in order to come up with a map of surface faulting and associated fractures in the Karonga area. We conducted both geological and geophysical techniques in the area. This article presents findings from geological techniques only.

The geological techniques aimed primarily at mapping the active fault(s) in order to delineate presence or absence of fault segments and fault kinematics. What are fault segments? Fault segments are discrete portions of given faults (McCalpin, 1996; Burbank and Anderson, 2001; Young et al., 2001). In their early stages of formation, fault segments occur as individual fault strands with displacement profiles that decrease from maximum in or near the center to zero at either tips (Burbank and Anderson, 2001; Young et al., 2001). Faults can grow by radial propagation (Cartwright et al., 1995; Burbank and Anderson, 2001), i.e. the individual fault segment simply lengthens and accumulates more displacement, while maintaining the standard displacement profiles. Faults can also grow by segment linkage when different individual fault segments become connected as they grow laterally, overlap and become hooked to each other on tips (Burbank and Anderson, 2001; Young et al., 2001) in a process which is referred to as fault interaction. Such interactions may promote or inhibit fault nucleation and growth, distort fault slip profiles, produce fault linkage and coalescence, and collectively result in populations of faults with distinctive characteristics (Peacock and Sanderson, 1991).

Although the processes by which segments form are still poorly understood (Vermilye and Scholz, 1999), seismotectonic studies show that it is commonly one or two fault segments that are involved in rupturing during large seismic events, each fault segment rupturing independently of the other, each with its own rupture history (Zhang et al., 1998). Large earthquakes, commonly of a characteristic size, repeatedly rupture the same part of segment of a fault, less commonly extending into adjacent segments (Schwartz and Coppersmith, 1984). Earthquakes may be termed "characteristic earthquakes" when they show repetition, break segments, rupturing the full width of the seismic zone and relieving the bulk stress on the fault segment they break (Kelleher et al., 1973; Schwartz and Coppersmith, 1984). Characteristic earthquakes should have comparable rupture extent, magnitude, and total slip. In other words, such earthquakes should have some regularity to their occurrence (Goes, 1996; McCalpin, 1996). According to McCalpin (1996), there is a relationship between the type of fault segment, its characteristics and the likelihood of that given fault segment being an earthquake segment (e.g. Wesnousky, 2008). Therefore, for evaluation of both past and future earthquakes, the study of fault segments using geologic data from paleoseismological sites (from both stratigraphic and geomorphic evidence) is essential (Piccardi, 2005). The study of fault segmentation is thus commonly used to estimate the potential earthquake size. Segment boundaries play an important role in arresting earthquake ruptures from event to event (Zhang et al., 1998).

2. Geological setting of the study area in Karonga

The study area is predominantly underlain by Precambrian to Lower Paleozoic metamorphic and igneous rocks that form the basement complex of Malawi. Overlying the basement complex are several patches of Karoo sediments and Cretaceous to Recent sediments such as lacustrine and fluvial sediments (Ray, 1975).

The basement complex is comprised mainly of gneisses (biotite and amphibolite gneisses, Fig. 2) and granitic intrusions of the Ubendian tectonic domain (ca. 2000 Ma) that extends from southern Tanzania into Malawi. The basement is intruded by dolerite and gabbroic dykes. Sandstones and shales with coal seams (Upper Carboniferous–Triassic), were deposited in basins extremely controlled by faults characterized by N–S and NW–SE trends (Ray, 1975). Cretaceous to Pleistocene Lacustrine sediments lie

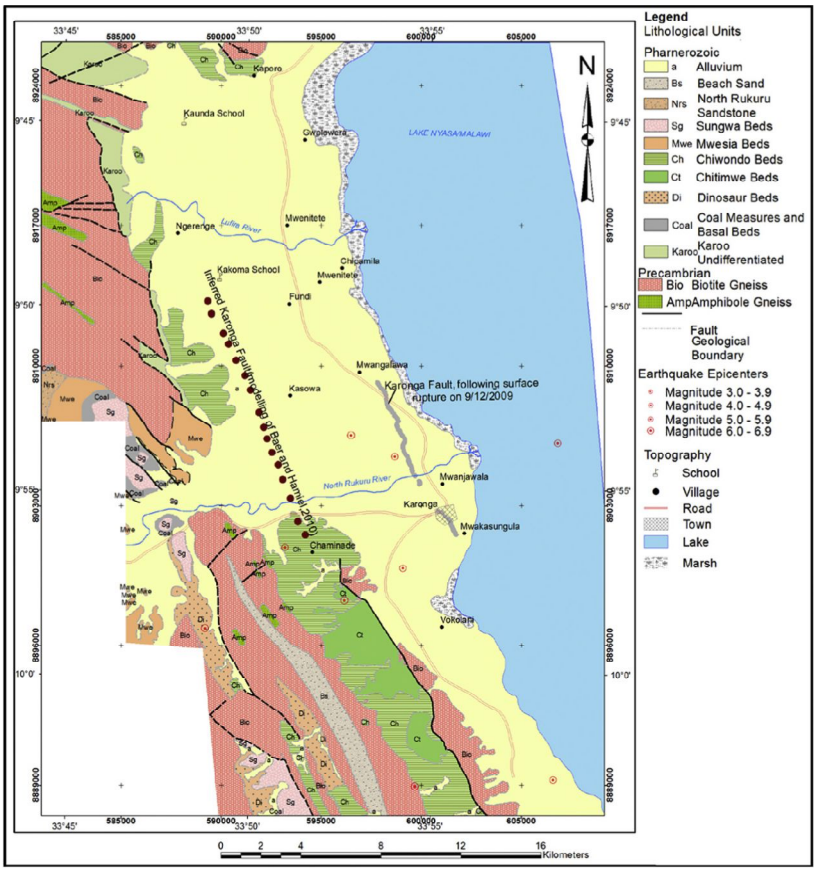


Fig. 2. Geological map of the study area (Karonga area), famously known as Ighembe-Lupembe area showing lithological units and associated faults in the area. The Karonga fault that caused the December 2009 earthquake is also shown in red as a thick line on the eastern side. Note the right-steps every about 1 km along the Karonga fault. Dotted lines refer to an inferred fault by Baer and Hamil (2010) and Biggs et al. (2010). No details are given on this dotted fault. The earthquakes with magnitudes are shown in filled circles (compare with Fig. 1).

unconformable on the basement complex gneisses. They include Dinosaur, Chiwondo, Chitimwe, Mwesia and Sungwa beds (Fig. 2). The lakeshore plain is dominantly covered by beach sands, alluvium and marsh deposits of Upper Pleistocene to Recent ages. Generally, the rift related structures are extremely important in controlling both the distribution of sediments in the basin as a whole and also details of sedimentation on a local scale (Crossley and Crow, 1980; Crossley, 1984).

According to Ebinger (1989) and Ring et al. (1992), there is a decrease in faulting activity from north of the Malawi rift due south as evidenced from degree of subsidence, sediment accumulation and rift-flank uplift. Ebinger (1989) show that rifting in this area started ca. 8 Ma.

In the Chitipa-Karonga area (Chitipa is about 85 km NW of Karonga, outside the study area), the basement complex is characterized by NW–SE structural trends and in the catchment area of South Rukuru River, N–S structural trends dominate the area. Rift faults affect all rock types in the area and they trend NW–NE and N–S (Malawi Geological Survey).

Table 1
Statistical fault parameters.

	N	Min	Max	Mean
Throw (cm)	60	0	43	11.9
Lateral displacement (cm)	16	0	12	3.72
Opening (cm)	56	1.5	40	10.8

The study area is situated on alluvium deposits, composed of sandy clays, terrace sands and gravels. According to borehole records drilled between 1961 and 1975 in the study area, depth to the basement complex increases from west to east. Around Mwenitete area (Fig. 2), borehole depths of up to 44 m were recorded. At such depths, the basement complex was not reached (Pers. Comm.).



Fig. 3a. Left-stepping fault strand at Karonga. A fault ends on the right near the person in white and another one emerges near the person in black to the left.



Fig. 3b. Left-stepping fault at Karonga.



Fig. 4b. Destructed Chensewe Primary School south of Karonga but no visible surface fractures. Temporary classrooms are erected (tents).

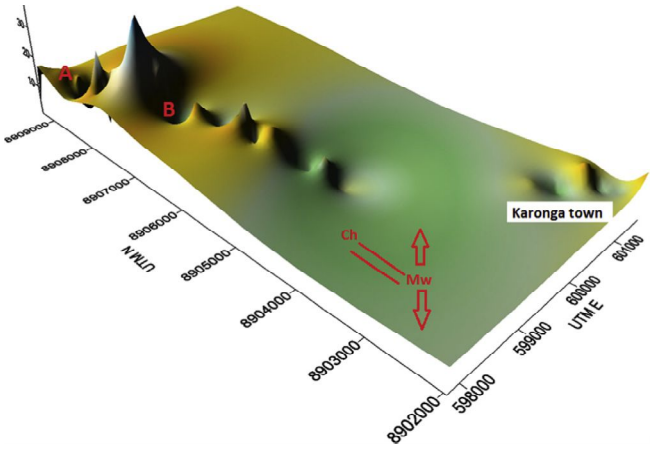


Fig. 4a. Perspective view of the Karonga fault showing the amount of throw in cm (as vertical axis) the fault trace from the Elias area to the northern end of the fault to Karonga town to the south. See the trace of the destructed zone, from Chensewe Primary School (Ch) to Mwanyongo village (Mw) shown in red where no fault trace was observed in the field. Note also the arrows point to the direction taken by sand boils (liquefaction); see the corresponding 'GAP' in Fig. 4c.

3. Methods used

Using the available geological map of the Karonga area on which preliminary faults/surface fractures were mapped, the active fault mapping was carried out as follows:

(a) The surface fractures were re-mapped (cross-checked) using <10-m resolution Garmin 12 hand GPS; xyz data (easting, northing and elevation) were recorded, (b) vertical displacements (vertical offset, VO), lateral displacements as well as amount of opening (horizontal separation between two blocks) were measured at various points using a 50-m tape measure, (c) using a geological compass, dip and strike, orientation and sense of movements were measured, and (d) information on sand boils (liquefaction) was recorded and direction of which was measured and fine-tuned on the basis of information obtained from local people.

These data were recorded on excel spread sheet, processed and statistical computations were performed in order to get representative fault parameters, mean values of throw or vertical offsets, lateral displacements and amount of opening. Each of these parameters was further plotted along the entire fault trace in order to obtain the 'along fault' displacement. The latter was used to estimate fault segments.

Sources of errors in the field were noted; they include errors due to (i) relatively low precision of hand GPS (about ±10 m), (ii) use of geological compass on soft displaced materials that can deform relatively easily during measurements, (iii) use of tape measure in non-smooth topography it could lead to incorrect readings, (iv) inclined faults at depth (normal faults) tend to be sub-vertical near the surface due to relatively low confining pressure near the surface as opposite blocks in the fault plane tend to be far apart and therefore making it difficult to estimate the actual vertical offset, lateral displacement and other fault parameters and (v) error due to timing in taking field measurements. In other words, measurements were made a year after the seismic event meaning that post-seismic events or fault creep could have affected our readings (e.g. Wells and Coppersmith, 1994). Furthermore, errors due to erosion could be considered.

4. The Karonga fault

The Karonga fault, is a normal fault; it generally trends N290°–N350° and close to the surface it dips at higher angles due west. Active fault mapping that was conducted on the southern half of the fault revealed that the fault has variable amounts of throw (vertical offset, VO) from 0 cm to 43 cm, mean VO ~12 cm. The maximum lateral displacement is 12 cm, with 3.7 cm as mean VO. The maximum opening is 40 cm, mean 10.8 cm (Table 1). In many places, the fault is left-stepping (Figs. 3a and 3b), the steps being within few meters to tenths of meters along rupture length. However, after every ~1 km, right-steps emerge (Figs. 2, 3a and 3b) and the resulting steps are generally separated by greater or equal to 100 m distance.

There are several gaps along the fault: the fault dies and reappears along its length. Around the North Rukuru River for example, the fault trace could not be seen on the ground (Fig. 2) but a 334° trending wide zone of destructed houses (from Chensewe Primary School to Mwanyongo village that are small villages within the Mwakasungula and Mwanjawala main villages) over 1 km long is not associated with any visible fault (Figs. 4a, 4b). This zone parallels the Karonga fault but the zone seems to lie somewhat west of the fault (Fig. 4a). There are several sand liquefactions

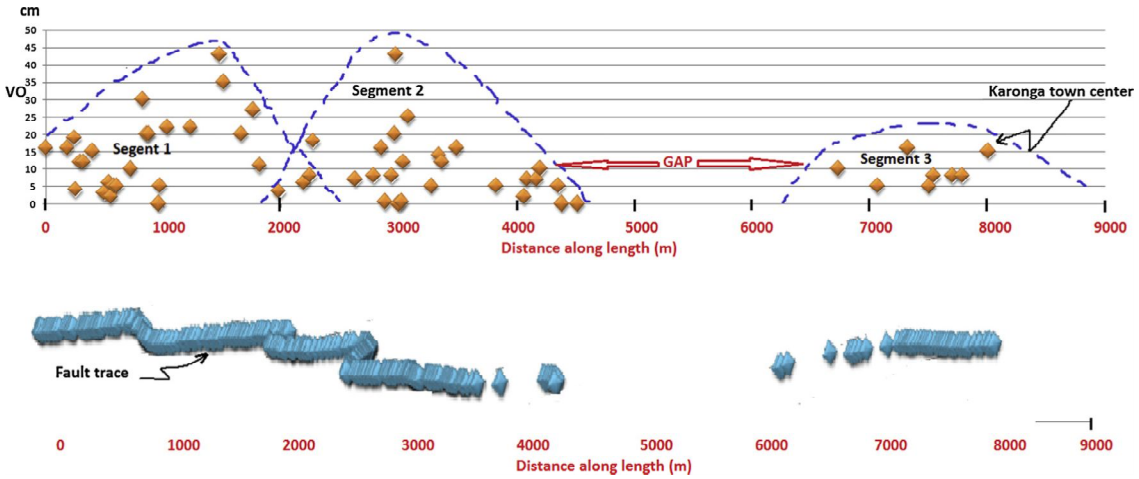


Fig. 4c. Along fault VO plot of the Karonga fault from the Elias area to the north (where the Malawi-Tanzania main road was cut across by the fault in December 2009) to Karonga town to the south. At least 3 fault segments can be seen from the plot, the forth one, inferred (not visible on the surface). Note that VO is represented by the vertical axis (cm) and length of fault is represented by the horizontal axis (m).

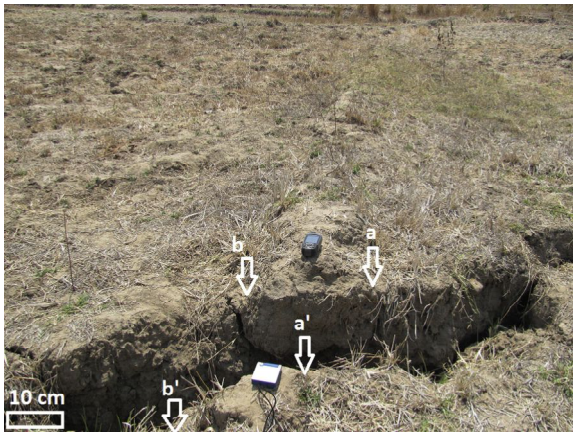


Fig. 5a. Both dip slip (obvious) and lateral/dextral movements (as indicated by points a–a′ and b–b′ that are thought to have been together before the rupture) along the Karonga fault trace.



Fig. 6. Dextral movement along the Karonga fault trace (5 cm displacement) at Karonga town. This is the SE wall. See the continuation of the fault southeasterly. Photo taken facing NE.



Fig. 5b. Dip slip movements as the main component. Note the amount of VO with reference to people standing on the footwall to the eastern side.

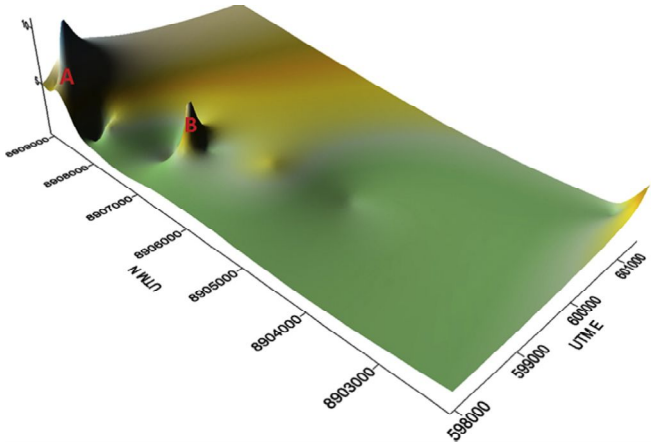


Fig. 7. Lateral displacement in cm (vertical axis) along the Karonga fault trace (compare with Figs. 4a and 4b).

along the Karonga fault, most or all of the sand liquefactions (visible and reported) are trending NE–SW, at higher angle to the general trend of the Karonga fault (Fig. 4a).

Based on the field observations, it can be interpreted that, (1) the Karonga fault is most likely made up at least 3 fault segments from its northern end to its southern part in Karonga

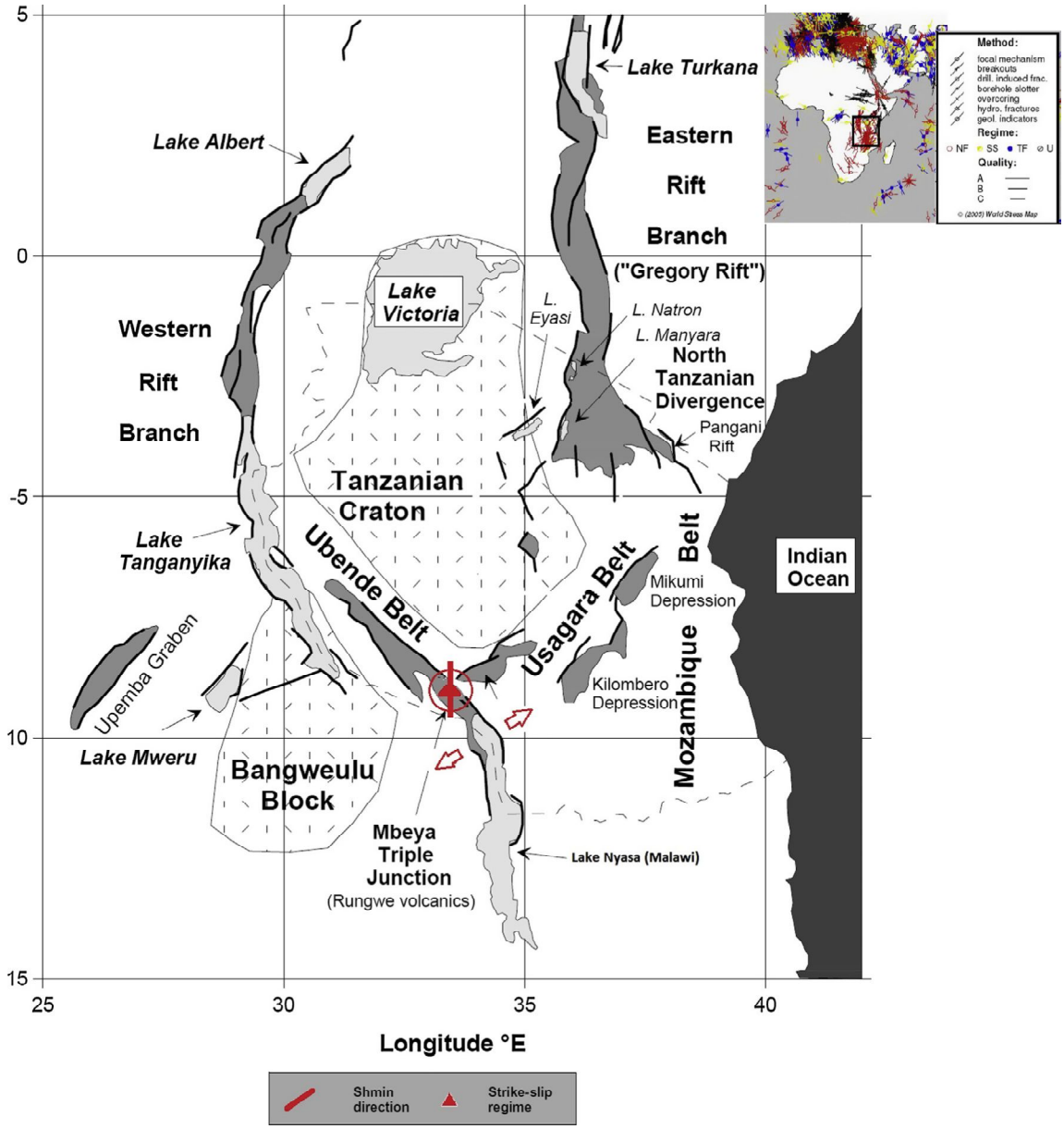


Fig. 8. Approximate location of the Rungwe volcanic province (RVP) shown by a circle. The horizontal principal extension (Shmin) direction and the stress regimes are shown according to the principle of the World Stress Map (Sperner et al., 2003). Arrows show direction of extension (After Delvaux, 1991; Morley, 1999; Macheyeki et al., 2008). An insert is from World Stress Map (Africa part), release 2005. Shown are maximum horizontal stress orientations for qualities A, B, C. Symbols indicate type of stress measurement. Colors correspond to tectonic regimes for stress indicators deduced from focal mechanism solutions: red indicates normal, yellow strike-slip and blue thrust faulting regimes (after Barth, 2007).

town (Figs. 4a and 4c, Table 3). The fault segments were obtained after plotting vertical offsets, VO versus length of fault rupture/trace (Fig. 4c). Figs. 4a and 4c show 3 maxima indicating 3 clear fault segments with a fourth probable segment indicated by a 'gap'; (2) the absence of visible fault in the small villages of Chensewe and Mwanyongo between Mwakasungula and Mwanjawala main villages while the houses are destructed in a NW–SE trend (trend of the ruptured surface), indicates that the fault moved during the December 2009 seismic event but was not exposed to the surface in this area; (3) the presence of both lateral and dip slip components on the Karonga fault indicate that the fault, though essentially dip slip, is partly oblique (Table 1, Figs. 5–7) and that the sense of lateral component is essentially dextral.

Field data show that generally, both vertical and lateral displacements at any point along the fault are proportional, i.e. higher values of vertical displacements correspond with higher values of lateral displacements along the fault. Mean vertical and lateral displacements values increase towards the north and decrease towards the south (Figs. 4a and 4c). It is interesting to note that highest lateral displacements occur at both ends of Segment 1, points A and B (Figs. 4a, 4c and 7), which most likely represents fault interaction at fault segment tips as the fault (fault segments) grow.

5. Discussion

The Karonga fault is essentially a dip slip fault but with lateral component(s) hence an oblique fault. Using the formulae of

Table 2
Detailed fault parameters of the Karonga fault.

Wpt	UTM_E	UTM_N	Elevation (m)	Long.	Lat.	VO (cm)	Lmvt (cm)	Op (cm)	Sense of movement	Dip (deg)	Strike (deg)	Trend (deg)
1	597935	8909090	490	33.89391	−9.87042	16	5	13	Dextral			338
2	598037	8908941	491	33.8939	−9.87043	16		7				
3	597802	8909302	491	33.89389	−9.87039	4						330
4	597805	8909294	486	33.89394	−9.87052	19		19				
5	597807	8909285	485	33.89398	−9.8706							
6	597811	8909279	487	33.89382	−9.87024							
7	597809	8909264	487	33.89377	−9.87017							
8	597814	8909261	486	33.89369	−9.87006							
9	597824	8909239	487	33.89425	−9.8709							
10	597835	8909225	486	33.8935	−9.86992							
11	597842	8909211	486	33.89433	−9.87099							
12	597846	8909207	486	33.89341	−9.86983							
13	597851	8909200	485	33.89439	−9.87106							
14	597858	8909189	486	33.89441	−9.87112							
15	597863	8909177	485	33.89336	−9.86976							
16	597868	8909171	486	33.89444	−9.87119							
17	597874	8909163	486	33.8933	−9.86969							
18	597880	8909156	486	33.89326	−9.86964							
19	597890	8909146	487	33.89449	−9.8713							
20	597911	8909130	486	33.89321	−9.86953							
21	597919	8909118	486	33.89456	−9.87139							
22	597925	8909110	486	33.89458	−9.87143							
23	597932	8909093	486	33.89315	−9.86943							
24	597933	8909089	486	33.89467	−9.87151							
25	597938	8909079	486	33.8931	−9.86937							
26	597942	8909070	486	33.89306	−9.86933							
27	597972	8909037	485	33.89474	−9.87158							
28	597980	8909027	486	33.893	−9.8692							
29	597987	8909019	486	33.89479	−9.87167							
30	597989	8909013	486	33.89483	−9.87174							
31	597992	8909005	485	33.89485	−9.87177							
32	597998	8908993	486	33.8929	−9.86908							
33	598005	8908983	485	33.89489	−9.87181							
34	598008	8908978	486	33.89491	−9.87184							
35	598018	8908970	486	33.89493	−9.87188							
36	598025	8908962	487	33.89497	−9.87192							
37	598031	8908952	487	33.89281	−9.86888							
38	598035	8908944	486	33.89503	−9.87201							
39	598042	8908936	486	33.89276	−9.86885							
40	598044	8908933	485	33.89278	−9.86872							
41	598046	8908928	486	33.89274	−9.86866							
42	598050	8908924	486	33.89523	−9.87214							
43	598057	8908914	486	33.89272	−9.86858							
44	598079	8908900	486	33.8927	−9.86851							
45	598091	8908885	486	33.89534	−9.87227							
46	598097	8908878	486	33.8954	−9.87234							
47	598107	8908859	486	33.89549	−9.87251	12	5					
48	598111	8908850	486	33.89553	−9.87259							
49	598118	8908843	486	33.89559	−9.87265							
50	598125	8908834	485	33.89565	−9.87273	12	7	15	Dextral			
51	598150	8908812	488	33.89588	−9.87293							
52	598165	8908793	487	33.89602	−9.8731							
53	598177	8908785	487	33.89613	−9.87317							
54	598180	8908779	488	33.89616	−9.87323	15	12	7				343
55	598184	8908762	488	33.89619	−9.87338							
56	598203	8908713	488	33.89637	−9.87382							
57	598207	8908698	488	33.8964	−9.87396							
58	598209	8908683	488	33.89642	−9.8741	3		2				200
59	598209	8908670	488	33.89642	−9.87421							
60	598203	8908645	488	33.89637	−9.87444							
61	598205	8908629	489	33.89639	−9.87458	6						190
62	598202	8908609	489	33.89636	−9.87477	2						
63	598212	8908584	489	33.89645	−9.87499	5		10				340
64	598217	8908559	489	33.8965	−9.87522	5		25				
65	598221	8908546	489	33.89654	−9.87533							
66	598228	8908534	489	33.8966	−9.87544							
67	598216	8908458	490	33.89649	−9.87613							
68	598220	8908431	488	33.89653	−9.87637	10		7				
69	598220	8908422	490	33.89653	−9.87646							
70	598218	8908415	489	33.89651	−9.87652							
71	598219	8908401	490	33.89652	−9.87665							
72	598220	8908394	490	33.89653	−9.87671							
73	598227	8908367	490	33.8966	−9.87695							
74	598227	8908367	490	33.8966	−9.87695							337

(*continued on next page*)

Table 2 (*continued*)

Wpt	UTM_E	UTM_N	Elevation (m)	Long.	Lat.	VO (cm)	Lmvt (cm)	Op (cm)	Sense of movement	Dip (deg)	Strike (deg)	Trend (deg)
75	598228	8908325	492	33.89661	−9.87733							
76	598230	8908323	489	33.89662	−9.87735	30		20				
77	598235	8908305	490	33.89667	−9.87751							
78	598237	8908298	490	33.89669	−9.87758							
79	598238	8908290	489	33.8967	−9.87765	20		10				
80	598241	8908272	490	33.89673	−9.87781	20	0	10				
81	598256	8908187	488	33.89686	−9.87858	0	0.5	12	Sinistral?			
82	598259	8908179	488	33.89689	−9.87865	5	3	5				
83	598265	8908163	488	33.89695	−9.8788							
84	598267	8908157	489	33.89697	−9.87885							
85	598271	8908147	488	33.897	−9.87894							
86	598277	8908133	488	33.89706	−9.87907							
87	598286	8908123	488	33.89714	−9.87916	22		15				
88	598290	8908101	488	33.89718	−9.87936							
89	598297	8908092	488	33.89724	−9.87944							
90	598312	8908081	488	33.89738	−9.87954							
91	598323	8908049	488	33.89748	−9.87983							
92	598334	8908033	488	33.89758	−9.87997							
93	598352	8908013	488	33.89774	−9.88015							
94	598377	8907999	488	33.89797	−9.88028							
95	598387	8907992	488	33.89806	−9.88034							
96	598392	8907987	489	33.89811	−9.88039							
97	598395	8907984	489	33.89814	−9.88041							
98	598398	8907981	488	33.89816	−9.88044							
99	598413	8907970	488	33.8983	−9.88054							
100	598419	8907961	488	33.89836	−9.88062	22		18				
101	598428	8907944	488	33.89844	−9.88077							
102	598442	8907921	488	33.89857	−9.88098							
103	598468	8907883	489	33.8988	−9.88132							
104	598473	8907876	488	33.89885	−9.88139							
105	598485	8907854	488	33.89896	−9.88159							
106	598491	8907840	488	33.89902	−9.88171							
107	598495	8907827	488	33.89905	−9.88183							
108	598504	8907816	488	33.89913	−9.88193							
109	598515	8907803	488	33.89924	−9.88205							
110	598522	8907796	488	33.8993	−9.88211							
111	598528	8907787	488	33.89935	−9.88219							
112	598547	8907770	488	33.89953	−9.88234							
113	598563	8907755	488	33.89967	−9.88248	43		15				
114	598575	8907735	488	33.89978	−9.88266							
115	598578	8907729	488	33.89981	−9.88271							
116	598581	8907727	488	33.89984	−9.88273	35		5		80	328	
117	598590	8907711	488	33.89992	−9.88288							
118	598599	8907691	488	33.9	−9.88306							
119	598610	8907682	488	33.9001	−9.88314							
120	598617	8907665	488	33.90017	−9.88329							
121	598624	8907656	488	33.90023	−9.88337							
122	598626	8907647	488	33.90025	−9.88345							
123	598629	8907638	488	33.90028	−9.88354							
124	598639	8907624	488	33.90037	−9.88366							
125	598643	8907614	488	33.90041	−9.88375							
126	598658	8907599	488	33.90054	−9.88389	20		40				
127	598666	8907590	489	33.90062	−9.88397							
128	598682	8907576	488	33.90076	−9.8841							
129	598688	8907570	488	33.90082	−9.88415							
130	598697	8907556	488	33.9009	−9.88428							
131	598706	8907548	488	33.90098	−9.88435							
132	598706	8907547	489	33.90098	−9.88436							
133	598715	8907537	489	33.90107	−9.88445							
134	598724	8907526	489	33.90115	−9.88455							
135	598728	8907517	488	33.90119	−9.88463	27		15				
136	598748	8907481	490	33.90137	−9.88495							
137	598754	8907471	490	33.90142	−9.88504	11						
138	598761	8907462	491	33.90149	−9.88512							
139	598779	8907438	490	33.90165	−9.88534							
140	598788	8907426	490	33.90173	−9.88545							
141	598794	8907409	489	33.90179	−9.8856							
142	598801	8907388	491	33.90183	−9.88576							
143	598798	8907392	491	33.90185	−9.88579							
144	598802	8907381	490	33.90186	−9.88586							
145	598807	8907369	491	33.90191	−9.88596							
146	598726	8907278	491	33.90117	−9.88679	3.5	0	10		88	330	4
147	598727	8907265	491	33.90118	−9.88691							
148	598729	8907223	492	33.9012	−9.88729							
149	598729	8907214	491	33.9012	−9.88737							

Table 2 (*continued*)

Wpt	UTM_E	UTM_N	Elevation (m)	Long.	Lat.	VO (cm)	Lmvt (cm)	Op (cm)	Sense of movement	Dip (deg)	Strike (deg)	Trend (deg)
150	598735	8907201	492	33.90126	−9.88749							
151	598749	8907173	492	33.90139	−9.88774							
152	598750	8907164	492	33.90139	−9.88782							
153	598758	8907139	492	33.90147	−9.88805							
154	598765	8907125	492	33.90153	−9.88817							
155	598768	8907116	492	33.90156	−9.88825							
156	598773	8907068	492	33.90161	−9.88869	6	2.5	10	Dextral			
157	598780	8907045	492	33.90167	−9.8889							
158	598801	8907022	492	33.90186	−9.8891	8		6				
159	598804	8907012	493	33.90189	−9.88919							
160	598805	8907011	492	33.9019	−9.8892							
161	598808	8907001	493	33.90193	−9.88929							
162	598812	8906996	492	33.90196	−9.88934	18	7.5	16	Dextral			162
163	598812	8906990	492	33.90196	−9.88939							
164	598815	8906974	491	33.90199	−9.88954							
165	598834	8906964	492	33.90217	−9.88963							
166	598836	8906951	492	33.90218	−9.88974							
167	598842	8906944	492	33.90224	−9.88981							
168	598843	8906937	492	33.90225	−9.88987							
169	598853	8906913	492	33.90234	−9.89009							
170	598860	8906909	492	33.9024	−9.89012							
171	598864	8906900	493	33.90244	−9.8902							
172	598866	8906895	492	33.90246	−9.89025							
173	598869	8906883	492	33.90249	−9.89036							
174	598872	8906874	493	33.90251	−9.89044							
175	598883	8906856	492	33.90262	−9.8906							
176	598886	8906849	492	33.90264	−9.89067							
177	598882	8906847	493	33.90261	−9.89068		2	3	Dextral			
178	598906	8906809	493	33.90283	−9.89103							
179	598930	8906784	491	33.90305	−9.89125							
180	598951	8906757	492	33.90324	−9.8915							
181	598965	8906740	492	33.90337	−9.89165							
182	598987	8906710	492	33.90357	−9.89192							
183	599002	8906689	492	33.9037	−9.89211	7		19				
184	599029	8906667	492	33.90395	−9.89231							
185	599032	8906660	492	33.90398	−9.89237							
186	599045	8906635	492	33.9041	−9.8926							
187	599060	8906630	492	33.90424	−9.89264							
188	599093	8906559	491	33.90454	−9.89328	8		5				350
189	599098	8906543	492	33.90458	−9.89343							
190	599104	8906531	492	33.90464	−9.89354							
191	599106	8906521	492	33.90466	−9.89363							
192	599110	8906516	493	33.90469	−9.89367							
193	599112	8906510	492	33.90471	−9.89373							
194	599118	8906497	493	33.90477	−9.89384	16		17				
195	599121	8906495	491	33.90479	−9.89386							
196	599121	8906484	491	33.90479	−9.89396							
197	599123	8906482	492	33.90481	−9.89398							
198	599122	8906463	491	33.9048	−9.89415	0.5		10				
199	599121	8906448	492	33.9048	−9.89429							
200	599118	8906432	492	33.90477	−9.89443							
201	599116	8906418	493	33.90475	−9.89456							
202	599113	8906408	493	33.90472	−9.89465							
203	599113	8906401	493	33.90472	−9.89471	8		5				
204	599100	8906378	493	33.90461	−9.89492							
205	599098	8906368	493	33.90459	−9.89501	20		8				
206	599095	8906354	494	33.90456	−9.89514	43		40				
207	599094	8906349	494	33.90455	−9.89518							
208	599094	8906346	494	33.90455	−9.89521							
209	599089	8906337	494	33.90451	−9.89529							
210	599086	8906328	494	33.90448	−9.89537							
211	599082	8906321	493	33.90439	−9.89544	0		1.5				211
212	599076	8906320	494	33.90444	−9.89544							
213	599074	8906311	494	33.90437	−9.89553							
214	599069	8906302	493	33.90433	−9.89561							
215	599066	8906296	495	33.9043	−9.89566							
216	599063	8906286	494	33.90427	−9.89575	0.5		15				
217	599061	8906282	494	33.90425	−9.89579							
218	599054	8906268	494	33.90419	−9.89592	12		15				200
219	599051	8906259	494	33.90416	−9.896							
220	599050	8906247	493	33.90415	−9.89611							
221	599034	8906226	494	33.90401	−9.8963							
222	599033	8906215	494	33.904	−9.89639	25		30				290
223	599033	8906216	493	33.904	−9.8964							
224	599029	8906204	492	33.90396	−9.89649							

(*continued on next page*)

Table 2 (*continued*)

Wpt	UTM_E	UTM_N	Elevation (m)	Long.	Lat.	VO (cm)	Lmvt (cm)	Op (cm)	Sense of movement	Dip (deg)	Strike (deg)	Trend (deg)
225	599029	8906190	494	33.90396	−9.89662							
226	599025	8906182	494	33.90393	−9.89669							
227	599027	8906171	493	33.90395	−9.89679							
228	599024	8906157	491	33.90392	−9.89692							
229	599025	8906148	494	33.90393	−9.897							
230	599025	8906144	493	33.90393	−9.89704							
231	599018	8906134	494	33.90386	−9.89713							
232	599020	8906112	493	33.90388	−9.89733							
233	599019	8906098	491	33.90387	−9.89745							
234	599017	8906074	493	33.90386	−9.89767							
235	599048	8906010	494	33.90414	−9.89825	5		5				334
236	599054	8906003	494	33.9042	−9.89831							
237	599063	8905981	494	33.90428	−9.89851							
238	599067	8905966	495	33.90432	−9.89865							
239	599078	8905953	495	33.90442	−9.89876	14		15				
240	599084	8905931	494	33.90447	−9.89896	12		6				
241	599087	8905926	495	33.9045	−9.89901							
242	599094	8905915	494	33.90456	−9.89911							
243	599100	8905907	494	33.90462	−9.89918							
244	599111	8905889	495	33.90472	−9.89934							
245	599113	8905880	495	33.90474	−9.89942							
246	599117	8905869	494	33.90477	−9.89952							
247	599123	8905858	494	33.90483	−9.89962							
248	599126	8905849	495	33.90486	−9.8997							
249	599133	8905834	495	33.90492	−9.89984							
250	599142	8905823	495	33.905	−9.89994							
251	599146	8905818	495	33.90504	−9.89998	16	3	10	Dextral			
252	599173	8905786	494	33.90529	−9.90027							
253	599174	8905784	496	33.9053	−9.90029							
254	599174	8905764	496	33.9053	−9.90047							
255	599179	8905752	495	33.90534	−9.90058							
256	599184	8905740	496	33.90539	−9.90069							
257	599187	8905733	495	33.90542	−9.90075							
258	599194	8905716	495	33.90548	−9.9009							
259	599200	8905702	495	33.90553	−9.90103							
260	599205	8905701	496	33.90558	−9.90104							
261	599207	8905696	496	33.9056	−9.90108							
262	599209	8905691	495	33.90562	−9.90113							
263	599211	8905685	496	33.90564	−9.90118							
264	599222	8905671	495	33.90574	−9.90131							
265	599237	8905654	496	33.90587	−9.90146							
266	599243	8905649	497	33.90593	−9.90151							
267	599244	8905640	496	33.90594	−9.90159							
268	599254	8905627	495	33.90603	−9.90171							
269	599259	8905625	496	33.90607	−9.90173							
270	599266	8905614	494	33.90614	−9.90182							
271	599269	8905604	496	33.90617	−9.90192							
272	599272	8905597	495	33.90619	−9.90198							
273	599272	8905590	497	33.90619	−9.90204							
274	599272	8905583	495	33.90619	−9.9021							
275	599272	8905580	494	33.90619	−9.90213							
276	599282	8905550	496	33.90629	−9.9024							
277	599284	8905536	496	33.90631	−9.90253							
278	599291	8905520	496	33.90637	−9.90267							
279	599290	8905514	495	33.90636	−9.90273	5		5				
280	599291	8905507	496	33.90637	−9.90279							
281	599287	8905496	496	33.90633	−9.90289							
282	599288	8905491	495	33.90634	−9.90294							
283	599290	8905480	495	33.90636	−9.90304							
284	599290	8905468	495	33.90636	−9.90314							
285	599293	8905461	494	33.90639	−9.90321							
286	599298	8905449	495	33.90643	−9.90332							
287	599299	8905445	495	33.90644	−9.90335							
288	599302	8905427	494	33.90647	−9.90352							
289	599307	8905413	496	33.90652	−9.90364							
290	599310	8905405	497	33.90655	−9.90371							
291	599336	8905383	495	33.90678	−9.90391							
292	599341	8905370	495	33.90683	−9.90403							
293	599342	8905367	494	33.90684	−9.90406							
294	599344	8905357	497	33.90686	−9.90415							
295	599346	8905350	496	33.90688	−9.90421							
296	599347	8905345	495	33.90688	−9.90426							
297	599351	8905338	497	33.90692	−9.90432							
298	599358	8905322	495	33.90699	−9.90446							
299	599363	8905318	496	33.90703	−9.9045							

Table 2 (*continued*)

Wpt	UTM_E	UTM_N	Elevation (m)	Long.	Lat.	VO (cm)	Lmvt (cm)	Op (cm)	Sense of movement	Dip (deg)	Strike (deg)	Trend (deg)
300	599365	8905305	495	33.90705	−9.90462							
301	599373	8905292	495	33.90712	−9.90473	2		3				
302	599378	8905279	496	33.90717	−9.90485							
303	599381	8905269	496	33.9072	−9.90494	7		7				
304	599391	8905251	495	33.90729	−9.9051							
305	599394	8905240	496	33.90732	−9.9052							
306	599413	8905195	496	33.90749	−9.90561	7		7				
307	599417	8905180	496	33.90753	−9.90575							
308	599420	8905169	496	33.90755	−9.90585							
309	599424	8905164	496	33.90759	−9.90589	10		18				
310	599428	8905146	497	33.90763	−9.90605							
311	599426	8905140	496	33.90761	−9.90611							
312	599430	8905127	496	33.90765	−9.90622							
313	599433	8905110	496	33.90767	−9.90638							
314	599438	8905101	496	33.90772	−9.90646							
315	599440	8905095	497	33.90774	−9.90651							
316	599443	8905091	497	33.90777	−9.90655							
317	599445	8905083	496	33.90778	−9.90662							
318	599446	8905077	496	33.90779	−9.90668							
319	599451	8905070	496	33.90784	−9.90674							
320	599473	8905018	495	33.90804	−9.90721	5		5				
321	599473	8905016	495	33.90804	−9.90723							
322	599476	8905004	496	33.90807	−9.90734							
323	599479	8904997	496	33.9081	−9.9074							
324	599487	8904991	495	33.90817	−9.90745	0		4				
325	599490	8904973	495	33.9082	−9.90762							
326	599493	8904959	495	33.90823	−9.90774							
327	599497	8904950	495	33.90826	−9.90782							
328	599499	8904935	496	33.90828	−9.90796							
329	599521	8904895	497	33.90848	−9.90832							
330	599536	8904869	498	33.90862	−9.90856	0	1	2	Sinistral?			
331	599538	8904856	496	33.90864	−9.90867							
332	599540	8904844	497	33.90866	−9.90878							
333	599624	8904714	495	33.90943	−9.90996							
334	599632	8904702	495	33.9095	−9.91006							
335	599808	8904480	492	33.91111	−9.91207							
336	599814	8904476	492	33.91117	−9.9121							
337	599823	8904459	492	33.91125	−9.91226							
338	599828	8904448	492	33.91129	−9.91236							
339	599834	8904436	491	33.91135	−9.91246							
340	599841	8904424	492	33.91141	−9.91257							
341	599844	8904410	492	33.91144	−9.9127							
342	599851	8904390	492	33.91151	−9.91288							
343	599854	8904374	492	33.91153	−9.91302							
344	599861	8904342	492	33.9116	−9.91331							
345	599848	8904291	492	33.91148	−9.91377							
346	600753	8902979	492	33.91977	−9.92562	10		3				295
347	600766	8902969	493	33.91989	−9.92571							
348	600792	8902956	493	33.92012	−9.92582							
349	600967	8902905	495	33.92172	−9.92628							330
350	601050	8902750	489	33.92248	−9.92768	5		10				330
351	601051	8902750	489	33.92249	−9.92768							
352	601062	8902735	489	33.92259	−9.92782							
353	601072	8902724	490	33.92268	−9.92792							
354	601089	8902712	490	33.92284	−9.92802							
355	601114	8902700	489	33.92307	−9.92813							
356	601202	8902639	490	33.92387	−9.92868							320
357	601250	8902592	489	33.92431	−9.9291							
358	601268	8902572	490	33.92448	−9.92929	16		5				320
359	601279	8902563	490	33.92458	−9.92937							
360	601287	8902544	489	33.92465	−9.92954							
361	601290	8902532	490	33.92468	−9.92965							
362	601295	8902525	490	33.92472	−9.92971							
363	601300	8902510	491	33.92477	−9.92985							
364	601308	8902493	489	33.92484	−9.93							
365	601323	8902477	489	33.92498	−9.93014							
366	601338	8902455	489	33.92512	−9.93034							
367	601347	8902432	489	33.9252	−9.93055							
368	601353	8902413	490	33.92525	−9.93072	5	2	5	Dextral			
369	601361	8902393	489	33.92533	−9.9309							
370	601369	8902379	488	33.9254	−9.93103	8		5				
371	601377	8902348	488	33.92548	−9.93131							
372	601395	8902299	489	33.92564	−9.93175							
373	601407	8902278	488	33.92575	−9.93194							
374	601414	8902266	488	33.92581	−9.93205							

(*continued on next page*)

Table 2 (*continued*)

Wpt	UTM_E	UTM_N	Elevation (m)	Long.	Lat.	VO (cm)	Lmvt (cm)	Op (cm)	Sense of movement	Dip (deg)	Strike (deg)	Trend (deg)
375	601419	8902257	488	33.92586	−9.93213							
376	601424	8902243	489	33.92591	−9.93226							
377	601430	8902234	487	33.92596	−9.93234							
378	601434	8902229	487	33.926	−9.93238	8	4	5				
379	601447	8902202	487	33.92612	−9.93263							
380	601457	8902172	488	33.92621	−9.9329							
381	601462	8902150	488	33.92626	−9.9331	8	5	2				
382	601468	8902140	487	33.92631	−9.93319							
383	601471	8902136	488	33.92634	−9.93322							
384	601487	8902109	488	33.92648	−9.93347							
385	601495	8902096	488	33.92656	−9.93358							
386	601506	8902063	488	33.92666	−9.93388							
387	601514	8902045	488	33.92673	−9.93404							
388	601523	8902026	488	33.92682	−9.93422							
389	601529	8902020	488	33.92687	−9.93427							
390	601555	8901988	489	33.92711	−9.93456							
391	601572	8901966	489	33.92726	−9.93476							
392	601573	8901959	489	33.92727	−9.93482	15		5				
393	601596	8901929	489	33.92748	−9.93509							
394	601609	8901908	489	33.9276	−9.93528							
395	601614	8901897	490	33.92765	−9.93538							
396	601630	8901840	490	33.9278	−9.9359							

ELV = Elevation from the mean seal level, VO = vertical displacement, Lmvt = Lateral displacement, Op = horizontal opening perpendicular to fault length, Wpt = GPS way pint.

McCalpin (1996),[1] and associated figures Figs. 9.2 and 9.3 and based on the historic earthquake of Bonilla et al. (1984) and Wells and Coppersmith (1994), it can be deduced that, for a maximum displacement of 43 cm (the highest value obtained in our study) to occur, the corresponding moment magnitude is supposed to be 6.42 (~Ms 6.4 ± 0.03) which corresponds to rupture length of about 14.30 km. It follows therefore that, the rupture length in the Karonga area was of the order of 14.30 km, about 1.6 times longer than what was actually observed/mapped (~9 km rupture length) during our field mission. By extrapolation, the fault would end around Chipamila village to the north (Fig. 2). The computed Mw = 6.4 ± 0.03 differs by Mw = 0.1 ± 0.03 from that of Biggs et al. (2010) who model this earthquake event to correspond to Mw = 6.3 (see inferred modeled fault from Biggs et al. (2010) west of the observed fault). The instrumental records on the 9th December 2009 earthquake are even lower by 0.2 ± 0.03 (Ms = 6.2). This can be explained by the fact that some of the 'foreshocks' could have contributed to this departure because although they were lower than the December 9 earthquake, they probably caused some surface deformations that culminated on 9th December 2009 to 43 cm. Thus any other 'aftershock(s)' could have caused some displacement which summed up to the observed 0.43 m (maximum) displacement.

The fact that the mean vertical and lateral displacement values increase towards the north and decrease towards the south as per Fig. 4a and 4c, imply that about 5.3 km was not mapped/observed on the surface towards the north (beyond Segment 1). These results are consistent with Ebinger et al. (1987, 1989), Ebinger (1989), and Ring et al. (1992) who show that magnitude of the East Africa Rift System faulting activities decrease due south.

This event has important structural implications, not only in terms of seismic hazard. The main interests of this event are:

- The earthquake sequence occurred on the shoaling side of the half graben, not along its master border fault, to the east of the lake.
- The event happened close to the Rungwe volcanic province (RVP), just south of it, but apparently did not involve magmatism/and dyking as in the Gelai case (Calais et al., 2008). In the latter, deformation was achieved by slow slip on a normal fault that promoted subsequent dyke intrusion by stress unclamping.
- Both the earthquake focal mechanisms and the surface ruptures show a dominant normal faulting mechanism, which is confirmed by the modeling of Biggs et al. (2010) and Hamiel et al. (2012). This area is just south of the Mbeya triple junction (the RVP) where Delvaux and Barth (2010) showed that the stress field is dominantly strike-slip, with a N–S direction of horizontal principal extension (Fig. 8). Therefore, this shows that the stress field of the RVP is not entirely continuing southwards but is essentially restricted to the RVP.
- The little lateral component or sense of movement associated with the Karonga-Malawi 19th December 2009 earthquake was essentially dextral, with insignificant (strike-slip) or sinistral components (see Table 2). Presence of both left-lateral at a local scale and right-lateral fault steps/échelon faults/fault strands at the regional scale has the following implications:
  - One: there are two tectonic stress fields responsible for each one of these échelon faulting mechanisms; an older event which was reactivated (most likely responsible for the left-stepping faults) and the younger event responsible for the December 9 2009 seismic event (most likely responsible for the right-stepping fault steps/strands). This argument is in line with Ring et al. (1992) who report stress perturbations with time.
  - Two: Both fault strands are co-genetic and were formed or re-activated during the seismic event of 9th December 2009. If indeed this happened, then, much more of the

[1] Earthquake magnitudes are currently reported as "moment magnitudes" (Mw),

$$Mw = \log(M0/1.5) - 10.73$$

and

$$Ms = \log 10(A/T) + 1.66 \log 10(\Delta) + 33$$

where M0 is the seismic moment given by the equation

$$M0 = \mu d a$$

where μ is the rigidity of a rock mass, i.e. the shear modulus of the crustal material involved in the rupture. It is taken as 3×1011 dyn/cm^2 (30 GPa) for the crust and 7×10^{11} dyn/cm^2 (70 GPa) for the upper mantle. The symbols d and a stand for average displacement and rupture area, respectively. The seismic moment is expressed either in dyn cm (cgs) or in N m (SI). The moment magnitude scale is related to the physical properties of the source. This scale does not saturate with large earthquakes (Shearer, 1999). '*A*' is displacement and '*T*' is the dominant period of the measured waves.

Table 3
Plot of computed moment magnitude, surface rupture length (computed) and maximum displacement (computed) along with observed surface rupture length. After McCalPin (1996), Figs. 9.2 and 9.3 and Bonilla et al. (1984) and Wells and Coppersmith (1994).

Moment magnitude (computed) Mw	Surface rupture length (observed) km	Surface rupture length (computed from computed moment magnitude) km	Maximum displacement (computed from computed moment magnitude) m	Comment
5.4	⩾2.0	2.00	0.020	Segment 1
5.5	⩾2.5	2.49	0.028	Segment 2
5.5	⩾2.5	2.49	0.028	Segment 3
5.3	⩾1.5	1.55	0.013	GAP (4th Segment?)
6.4	~9.0	14.29	0.432	Whole fault trace

fault sliding would have been inhibited in the left-steps (e.g. Harris et al., 1991). According to Harris et al. (1991), '...for left steps in right-lateral (dextral) shear, normal-traction on the overlapping crack tips increases, thereby inhibiting frictional sliding.' In Fig. 4c (between Segment 1 and 2) we observe a nearly 0.5 km fault overlap. However, it has to be stressed here that although the faulting mechanism is not strike-slip, it is not entirely normal faulting but rather oblique with lateral displacement of up to 12 cm (oblique fault).

- Biggs et al. (2010) do not report surface ruptures and their interferograms are not clear about this possibility. However, in their best models are all consistent with a rupture that "either broke or came close to the surface". Hamiel et al. (2012) however, report an observed 18 km surface fracture length, about 26% longer than what we report (14.30 km).

6. Conclusion and recommendations

The Karonga fault is not a pure normal fault; it has both dip and lateral components, the dip slip component is more prominent than the latter. Dextral and sinistral components are present, the latter is insignificant. The Karonga fault is segmented, 3 segments more evident, whereas the fourth one is not yet exposed to the surface. Although field mapping show only 9 km of surface rupture, maximum vertical offset of about 43 cm imply that the surface rupture was in little excess of 14 km that corresponds with Mw = 6.4. This implies that most or all segments over that distance (including the 'gap') could have moved during the 9th December 2009 Karonga earthquake.

For better analysis and assessment of the seismic hazard of the Karonga fault, we recommend similar study to be undertaken to the northern half of the Karonga fault. We further recommend the integration of paleoseismology and InSAR – Interferometry studies in order to better understand the fault history, reason for having both left-lateral and right-lateral échelon faults in one fault system, faults mechanism and other behavior of the fault(s) for better urban planning in this area.

Acknowledgements

Authors are indebted to IPPS for financial support. We also thank Dr. D. Delvaux of the Royal Museum for Central Africa – Belgium and Jonathan Kashabano of the Geological Survey of Tanzania for their constructive comments. Thanks are also due to the Karonga people who gave us support during filed mission in 2010. Thanks to Prof. Cynthia Ebinger and Prof. Shukrani Manya for their constructive comments to the manuscript. An anonymous reviewer is similarly thanked for the useful comments. Authors are indebted to Desdery Mujuni from the Geological Survey of Tanzania for improving Fig. 2.

References

Baer, G., Hamil, Y., 2010. East African Rifting Events Revealed by InSAR 2007 Gelai, Tanzania and 2009 Karonga, Malawi. Presentation made at the Geological Survey of Malawi.
Barth, A., 2007. Frequency sensitive moment tensor inversion for light to moderate magnitude earthquakes in eastern Africa and derivation of the regional stress _field. PhD Thesis. University at Karlsruhe (TH).
Biggs, J., Nissen, E., Craig, T., Jackson, J., Robinson, D.P., 2010. Breaking up the hanging wall of a rift-border fault: the 2009 Karonga earthquakes, Malawi. Geophys. Res. Lett. 37, L11305. http://dx.doi.org/10.1029/2010GL043179.
Bonilla, M.G., Mark, R.K., Leinkaemper, J.J., 1984. Statistical relations among earthquake magnitude, surface rupture, and surface fault displacement. Bull. Seismol. Soc. Am. 74, 2374–2411.
Burbank, D.W., Anderson, R.S., 2001. Tectonic Geomorphology. Blackwell Science, USA, pp: 33, 43, pp. 105–129.
Calais, E., d'Oreye, N., Albaric, J., Deschamps, A., Delvaux, D., Déverchere, J., Ebinger, C., Ferdinand, R.W., Kervyn, F., Macheyeki, A.S., Oyen, A., Perrot, J., Saria, E., Smets, B., Stamps, D.S., Wauthier, C., 2008. Strain accommodation by slow slip and dyking in a youthful continental rift, East Africa. Nature 456, 783–787. http://dx.doi.org/10.1038/nature07478.
Cartwright, J.A., Trudgill, B.D., Mansfield, C.S., 1995. Fault growth by segment linkage: an explanation for scatter in maximum displacement and trace length data from the Canyonlands grabens of SE Utah. J. Struct. Geol. 17, 1319–1326.
Crossley, R., 1984. Controls of sedimentation in the Malawi Rift valley, Central Africa. Sed. Geol. 40, 33–50.
Crossley, R., Crow, M.J., 1980. The Malawi rift. In: Geodynamic Evolution of the Afro-Arabian Rift System. Accademia Nationale Dei Lincei, Rome, pp. 78–88.
Delvaux, D., 1991. The Karoo to recent rifting in the western branch of the East-African Rift System: a bibliographical synthesis. Musee Roy. Afr. Central Tervuren (Dép. Géol. Min., Rap. Ann.) 1989–1990, 63–83.
Delvaux, D., Barth, A., 2010. African stress pattern from formal inversion of focal mechanism data. Implications for rifting dynamics. Tectonophysics 482, 105–128.
Ebinger, C.J., 1989. Geometric and kinematic development of boulder fault and accommodation zones, Kivu-Rusizi rift-Africa. Tectonics 8 (1), 117–133.
Ebinger, C.J., Rosendahl, B.R., Reynolds, D., 1987. Tectonic model of the Malawi rift, Africa. Tectonophysics 141, 215–235.
Ebinger, C.J., Bechtel, T.D., Forsyth, D.W., Bowin, C.O., 1989. Effective elastic plate thickness beneath the East African and Afar domes. J. Geophys. Res. 94, 883–896.
Goes, S.D.B., 1996. Irregular recurrence of large earthquakes: an analysis of historic and paleoseismic catalogs. J. Geophys. Res. 101B3, 5739–5749.
Hamiel, Y., Baer, G., Kalindekafe, L., Dombola, K., Chindandali, P., 2012. Seismic and aseismic slip evolution and deformation associated with the 2009–2010 northern Malawi earthquake swarm, East African Rift. Geophys. J. Int. 191, 898–908. http://dx.doi.org/10.1111/j.1365-246X.2012.05673.x.
Harris, R.A., Archuleta, R.J., Day, S.M., 1991. Fault steps and the dynamic rupture process: 2-D numerical simulations of a spontaneous propagating shear fracture. J. Geophys. Res. 18 (5), 893–896.
Kelleher, J.A., Sykes, L.R., Oliver, J., 1973. Possible criteria for predicting earthquake locations to major plate boundaries of Pacific and Caribbean. J. Geophys. Res. 78, 2547–2585.
Macheyeki, A.S., Delvaux, D., De Batist, M., Mruma, A., 2008. Fault kinematics and tectonic stress in the seismically active Manyara-Dodoma rift branch in Central Tanzania – Implications for the East African Rift. J. Afr. Earth Sci. 51, 163–188.
Malawi Geological Survey, 2009. Geological Map of Ighembe – Lupembe.
McCalpin, J.P. (Ed.), 1996. Paleoseismology. Academic Press, New York, 583 pp.
Morley, C.K., 1999. Geoscience of rift systems – evolution of East Africa. Am. Assoc. Petrol. Geol. Stud. Geol. 44, 242.
Peacock, D.C.P., Sanderson, D.J., 1991. Displacements, segment linkage and relay ramps in normal fault zones. J. Struct. Geol. 13 (6), 721–733.

Piccardi, L., 2005. Paleoseismic evidence of legendary earthquakes: the apparition of Archangel Michael at Monte Sant'Angelo (Italy). Tectonophysics 408, 113–128.

Ray, G.E., 1975. The Geology of the Chitipa – Karonga Area, Bulletin No. 42, Geological Survey Department, Malawi.

Ring, U., Betzler, C., Delvaux, D., 1992. Normal vs. strike-slip faulting during rift development in East Africa: the Malawi rift. Geology 20, 1015–1018.

Schwartz, D.P., Coppersmith, K.J., 1984. Fault behavior and characteristic earthquakes: examples from Wasatch and San Andreas Fault zone. J. Geophys. Res. 89, 5681–5698.

Shearer, P.M., 1999. Introduction to seismology. Cambridge University Press, UK, 260p.

Sperner, B., Müller, B., Heidbach, O., Delvaux, D., Reinecker, J., Fuchs, K., 2003. Tectonic stress in the Earth's crust: advances in the World Stress Map project. In: Nieuwland, D. (Ed.), New Insights into Structural Interpretation and Modeling. Geol. Soc. London Spec. Pub. 212, pp. 101–116.

Vermilye, J.M., Scholz, C.H., 1999. Fault propagation and segmentation: insight from the microstructural examination of a small fault. J. Struct. Geol. 21, 1623–1636.

Wells, D.L., Coppersmith, K.J., 1994. New empirical relations among magnitude, rupture length, rupture width, rupture area and surface displacement. Bull. Geol. Seismol. Soc. Am. 84, 974–1002.

Wesnousky, S., 2008. Displacement and geometrical characteristics of earthquake surface ruptures: issues and implications for seismic-hazard analysis and process of earthquake rupture. Bull. Seismol. Soc. Am. 98 (4), 1609–1632.

Young, M.J., Gawthorpe, R.L., Hardy, S., 2001. Growth and Linkage of a segment normal fault zone; the Late Jurassic Murchison-Statfjord North Fault, northern North Sea. J. Struct. Geol. 23, 1943–1952.

Zhang, P., Mao, F., Slemmons, D.B., 1998. Rupture terminations and size of segment boundaries from historical earthquake ruptures in the Basin and Range Province. Tectonophysics 308, 37–52.